JOURNAL OF SOLID STATE CHEMISTRY 50, 153–162 (1983)

An Investigation of the Coordination Number of Ni^{2+} in Nickel Bearing Phyllosilicates Using Diffuse Reflectance Spectroscopy

M. ISABEL TEJEDOR-TEJEDOR* AND MARC A. ANDERSON

Water Chemistry Program, 660 North Park Street, University of Wisconsin, Madison, Wisconsin 53706

AND ADRIEN J. HERBILLON

Section de Physico-Chimie Minérale du Musée Royal de l'Afrique Centrale and Université Catholique de Louvain, Place Croix du Sud 1, B 1348 Louvain-la-Neuve, Belgium

Received April 18, 1983; in revised form July 7, 1983

Visible region reflectance spectroscopy and nonlinear regression analysis of spectral data have been used to present qualitative and semiquantitative evidence that some tetrahedral Ni^{2+} is present in all six phyllosilicates examined. Highly crystalline willemseite and chrysotile, poorly crystalline nepouite as well as two natural minerals, and a mixture of poorly crystalline nepouite and nickel hydroxide all showed the presence of tetrahedral Ni^{2+} as well as octahedral nickel. Chemical analysis of willemseite confirmed quantitatively the presence of excess Ni lending further support for the presence of tetrahedral nickel.

Introduction

Recent papers and reviews concerning structure and crystal chemistry of Ni-bearing phyllosilicates reveal several particular traits which clearly distinguish these minerals from their pure Mg-bearing homologs (*1–3*). Regardless of whether these minerals belong to 1 : 1 (7 Å) or to 2 : 1 (10 Å) mineral families, it has often been noticed that atomic substitution of octahedral Mg^{2+} by Ni^{2+} cations in such frameworks is accompanied by modifications less often observed in pure magnesium end members of those families. For example, secondary Ni clay minerals generally have structural disorders and may deviate from theoretical stoichiometry (*2, 4*). In addition, we have seen that, particularly among 2 : 1 Ni silicates belonging to the kerolite–pimelite series, some specimens swell in presence of polar liquids. It is for this swelling characteristic that pimelites have sometimes been considered as belonging to the smectite group of clay minerals. In contrast, Brindley (*2*) considers these kerolite–pimelite minerals to be members of the 2 : 1 nonswelling layer silicate group. Brindley (*2*) does not, however, rule out the possibility that some specimens might consist of 2 : 1 nonswelling layers slightly interstratified with 2 : 1 swelling smectitelike layers.

Since capacity to swell is directly related to the number and nature of hydrated cat-

* To whom correspondence should be addressed.

0022-4596/83/ $3.00

ions present in interlamellar space and therefore to negative charge existing in the framework of these silicates, such observations regarding swelling in minerals containing Ni^{2+}, Mg^{2+}, and Si^{4+} as the only cations raise questions concerning the origin of charge. Indeed, isomorphic replacement of Mg^{2+} by Ni^{2+} in octahedral sheets of "talc-like" minerals should a priori have no effect on total charge balance and cannot therefore explain the induction of swelling behavior. Should, however, a small portion of Ni^{2+} occupy tetrahedral positions within the silica sheet, this would give rise to a net negative charge excess and related swelling properties. More generally, existence of tetrahedral Ni in layer silicates would also offer an alternative approach to considering the crystal chemistry of these silicates, whether or not they exhibit swelling properties. In this paper, we address this latter possibility and present evidence that Ni^{2+} may indeed be incorporated into tetrahedral sheets of various Ni bearing phyllosilicates.

Theory

Visible–ultraviolet absorption spectrum of tetrahedrally coordinated transition cations shows much more intensity than the corresponding spectrum for octahedrally coordinated cations. Therefore, it would seem possible to use diffuse reflectance spectroscopy as a technique to identify tetrahedrally coordinated Ni^{2+} in the presence of large amounts of octahedrally coordinated Ni (*5, 6*).

Although diffuse reflectance and optical absorption techniques used in examination of garnierites have indicated possible Ni^{2+} substitution for Mg^{2+} in octahedral positions (*1, 7, 8*), these studies were only based on absorption band energy analysis. To distinguish tetrahedral in the presence of octahedral Ni^{2+}, it is necessary to compare both band position and relative band intensity. We use this type of analysis to demonstrate that Ni^{2+} may be incorporated into tetrahedral as well as octahedral sheets.

Ni^{2+} Octahedral Spectrum

Spectrum for octahedrally coordinated Ni^{2+} can be interpreted by referring to energy level diagrams for the d^8 ion in an octahedral field. These transitions are spin-allowed:

$$^3A_{2g}(F) \text{ ---------- } ^3T_{2g}(F) \quad \text{near ir} \quad (1)$$

$$^3A_{2g}(F) \text{ ---------- } ^3T_{1g}(F) \quad \text{V–near ir} \quad (2)$$

$$^3A_{2g}(F) \text{ ---------- } ^3T_{1g}(P) \quad \text{V–uv.} \quad (3)$$

Following Lows' (*10*) suggestion, it is expected that the $^3F \rightarrow {}^3P$ transition would show a more intense spectrum than those corresponding to transitions between Stark levels. (It should be noted that all of these transitions have to be regarded as spin-allowed, Laporte-forbidden (*9*).

Ni^{2+} Tetrahedral Spectrum

Energy level diagrams for d^8 ions in tetrahedrally coordinated Ni^{2+} fields show that the most intense bands in the spectrum correspond to three spin-allowed transitions from a $^3T_1$ ground term:

$$^3T_1(F) \text{ ---------- } ^3T_2(F) \quad \text{ir} \quad (4)$$

$$^3T_1(F) \text{ ---------- } ^3A_2(F) \quad \text{near ir} \quad (5)$$

$$^3T_1(F) \text{ ---------- } ^3T_1(P) \quad \text{V} \quad (6)$$

Band intensities in tetrahedral complexes are higher than in octahedral ones because of *d–p mixing*. Although extinction coefficients have been reported to be around 100 (*9*), wide variations in this figure have been documented. Compared to intensities of spin-allowed, Laporte-forbidden transitions, spin-allowed Laporte-forbidden with *d–p mixing* transitions have one order magnitude higher extinction coefficients (*9*).

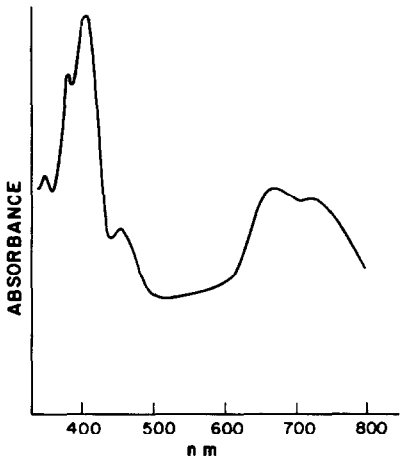

FIG. 1. Optical spectrum of Ni^{2+} in MgO, Ref. (*10*).

Spectral Evidence for Tetrahedral Ni^{2+} in Nickel Phyllosilicates

Normally, we would expect Ni^{2+} to appear in the brucite layer of phyllosilicates and therefore occupy a octahedrally coordinated position. Its spectrum in this case should be similar to the one reported by Low (*10*) for Ni^{2+} in magnesium oxides and illustrated here in Fig. 1 (*10*). Characteristically this spectrum shows two major bands over the energy regions we are concerned with here. The first broad band is a partially resolved doublet having a center of gravity at 680 nm. This doublet band results from the $^3A_{2g}(F) \rightarrow {}^3T_{1g}(F)$ transition mentioned previously for octahedral Ni^{2+} but also from a $^3A_{2g}(F) \rightarrow {}^1E_g(D)$ transition which, in spite of being partially forbidden, shows anomalously large intensity due to mixing of the ^1E_g and $^3T_{1g}$ levels because of spin/orbital interactions. The second more intense band occurs at 408 nm and corresponds to the $^3A_{2g}(F) \rightarrow {}^3T_{1g}(P)$ transition of octahedral Ni^{2+}. These transitions are summarized in Fig. 2.

If Ni^{2+} were to be placed in a slightly distorted octahedral field or the field were to show a lack of symmetry due to a difference in ligands, we would expect pertubations in the above spectrum. These perturbations have been studied by Schmitz-DuMont *et al.* (*11*) who investigated the influence of framework expansion on reflectance spectra for both tetrahedral and octahedral Ni^{2+} in oxo compounds. They observed that a reduction in symmetry causes little effect on ligand field components when ligands are at vertices of a regular octahedron. These authors found that this reduction produces ligand field weakening and results in a shift in band position towards slightly higher wavelength than that corresponding to a cubic field. Similar effects occasionally occur in framework or lattice expansion. On the other hand, distortion of the octahedron gives larger shifts (towards higher wavelength) than either lattice expansion or degree of symmetry perturbations. Wood (*12*) and Rossman *et al.* (*13*) have also shown that distortion not only gives the highest values for band wavelengths, but also more intense absorption bands, due to the fact that these cations are located in noncentrosymmetric sites. A summary of reported reflectance spectroscopic data is shown in Table I.

If, on the other hand, some Ni^{2+} were tetrahedrally coordinated in silicate layer,

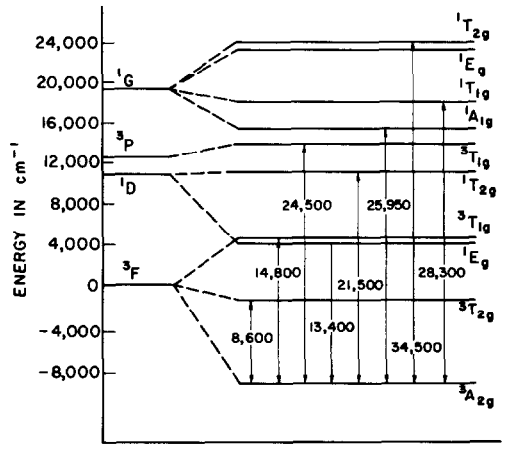

FIG. 2. Energy level diagram and observed optical transitions for Ni^{2+} in an octahedral field of MgO.

TABLE I

LITERATURE VALUES FOR Ni^{2+} TETRAHEDRAL AND OCTAHEDRAL TRANSITIONS AND THEIR RELATIVE INTENSITIES

Ni^{2+} octahedral			Ni^{2+} tetrahedral		Ni^{2+} octahedral + Ni^{2+} tetrahedral		
Compound	λ(nm)	${}^{I}\lambda_3/{}^{I}\lambda_2$	Compound	λ(nm)	Compound	λ(nm)	${}^{I}Oc\lambda_3/({}^{I}T\lambda_3 + {}^{I}Oc\lambda_2)$
$Ni(H_2O)_6^{2+}$ [a]	$\lambda_2 = 690$ $\lambda_3 = 395$	2	$Ni_{0.1}Zn_{1.9}SiO_4$ [c]	λ_3 { 637 581	$Ni_{0.1}Mg_{0.9}Al_2O_4$ [c]	λ_{3T} { 637 λ_2Oc { 599 λ_3Oc = 370	1.1
Various complexes [b] in solutions	— —	3–2	$Ni_{0.001}Zn_{0.999}O$ [c]	λ_3 { 662 621			
$Ni_{0.1}Mg_{0.90}O$ [c]	$\lambda_2 = 666$ $\lambda_3 = 417$	2.0			$Ni_{0.1}Mg_{0.9}Ga_2O_4$ [c]	λ_{3T} { 634 λ_2Oc { λ_3Oc = 392	1.2
$Ni_{0.01}Mg_{0.69}Zn_{0.3}O$ [c]	$\lambda_2 = 680$ $\lambda_3 = 410$	1.8					
$Ni_{0.25}Mg_{1.75}SiO_4$ [c]	$\lambda_2 = 770$ $\lambda_3 = 425$	1.6					
$(Mg_{0.9}Ni_{0.1})_2SiO_4$ [d]	$\lambda_2 = 680$						
Site 1	$\lambda_3 = 400$	1.1					
Site 2	$\lambda_2 = 780$ $\lambda_3 = 427$						
$Ni_{0.1}Mg_{0.9}TiO_3$ [c]	$\lambda^2 = 883$ $\lambda_3 = 454$	1.2					

[a] Ref. (*15*), p. 894.
[b] Ref. (*10*).
[c] Ref. (*11*).
[d] Ref. (*12*).

TABLE II

SAMPLE CHARACTERISTICS

Sample[b]	% Ni^{2+}/ Σ octahedral metal	Phases	CEC (meq/100 g)	^{S}BET (m^2/g)	Ni/Si ratio
A	55	Mg–Ni pimelite partially swellable	0.2 Ni	136	—
B	66	Mg–Ni pimelite partially swellable + serpentine	2.8 Ni 15.5 Mg	180	—
C	100	Willemseite[c]	—		0.82[a]
		2.13 free SiO_2	—	49.8	
D	100	Chrysotile	—	39.8	
E	100	Nepouite	—	—	—
F	Sample E before recrystallizing by hydrothermal reaction		—	—	—

[a] After removing the free SiO_2.
[b] In all samples the oxidation state of Ni was found to be 2+.
[c] This is the Ni talc synthetized by Martin *et al.* (*14*).

we might expect that a Ni^{2+} tetrahedral doublet band having a center of gravity between 610 and 640 nm would show contributions in the uv–visible spectra. This contribution would correspond to the relative percentage of Ni^{2+} tetrahedral/Ni^{2+} octahedral in the mineral. Thus one might see a shift in the broad Ni^{2+} octahedral doublet to higher wave numbers and a change in the relative intensities of the bands which would otherwise occur at 680 and 408 nm.

Experimental

General Requirements

Minerals were selected for their capacity to swell and for the absence of cations other than Ni, Mg, and Si. Using these constraints, the work presented here was performed on two selected natural phyllosilicates as well as on four synthetic samples, on Ni end member "talc-like" silicate (willemseite) and two different serpentines, and a mixture of nickel hydroxide/serpentine, both poorly crystalline (all characteristics of these minerals are summarized in Table II).

Techniques

X-ray diffraction was performed using Ni filtered Cu$K\alpha$ radiation. For the natural minerals, these studies have been done on untreated, K-saturated and ethylene glycol solvated samples, prepared as oriented aggregates. The synthetic samples were examined as random powder.

Analytical electron microscopy (A SEM 100 CX TEMSCAN fitted with a KEVEX energy dispersive spectrometer) including transmission electron microscopy and thin film X-ray microanalysis studies have been performed on the synthetic samples to check morphology and degree of homogeneity.

Oxidation number of Ni was determined using an iodometric method. In this case, samples were dissolved in a mixture of H_2SO_4–HF acids, in the presence of KI at 60°C under N_2. Blanks subjected to the same treatment as samples were titrated as well. Chemical analyses were done on the synthetic "talc-like" sample (willemseite) to determine accurately the Ni/Si ratio. This particular sample was subjected to alkaline fusion, with Na_2CO_3 + K_2CO_3 in Pt crucibles and collected with HCl acid. Af-

TABLE III

MAJOR BANDS AND RELATIVE INTENSITIES IN EXPERIMENTAL REFLECTANCE SPECTRA

Sample	Observed bands λ (nm)	$^{I}\lambda_3/^{I}\lambda_2$
A	735 (shoulder) 700 (shoulder) 658 (λ_2) 385 (λ_3)	1.08
B	740 (shoulder) 710 (shoulder) 660 (λ_2) 405 (shoulder) 385 (λ_3)	1.17
C	710 (shoulder) 740 (shoulder) 650 (λ_2) 385 (λ_3)	0.93
D	730 (shoulder) 695 (shoulder) 660 (λ_2) 390 (λ_3)	0.79
E	740 (shoulder) 665 (λ_2) 420 (shoulder) 395 (λ_3)	1.16
F	730 (shoulder) 710 (shoulder) 665 (λ_2) 395 (λ_3)	1.16

ter drying the suspension in a steam bath, the residue was treated with a mixture of HCl and HNO_3 acids to extract totally Ni from the SiO_2 precipitate. Amount of Si in the precipitate was determined gravimetrically and Si in solution was determined colorimetrically. Dissolved Ni was determined by atomic absorption from the resulting solution. A summary of the above results as well as surface areas for some of the minerals can be found in Table II.

Optical spectra were scanned on a Beckman Acta IV spectrophotometer with a diffuse reflectance accessory, in the wavelength range from 800 to 350 nm. Spectra were of powdered samples at room temperature with MgO used as a reflectance standard.

Results and Discussion

Reflectance bands and their relative intensities are collected in Table III. An inspection of the spectra, Fig. 3, shows that there are two relatively intense bands in the regions of 665–650 and 395–385 nm. The ratio of these band intensities (measured from peak areas), I_1/I_2, is not a constant for all of the spectra but changes from 1.16 to 0.79.

As suggested in the theory above, obvious assignment of the highest energy band in all spectra (400 nm) should be assigned to the transition $^3A_{2g}(F) \rightarrow {}^3T_{1g}(P)$ for Ni^{2+} in octahedral symmetry. However, the broad absorption with a band maxima around 666 nm necessitates some caution in its interpretation because it lies in an energy region too high to arise from the $^3A_{2g}(F) \rightarrow {}^3T_{1g}(F)$ transition and it furthermore shows an

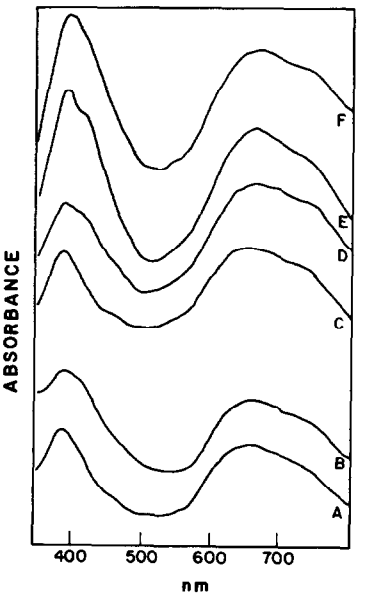

FIG. 3. uv reflectance spectra of phyllosilicates Reflectance spectra of phyllosilicates samples A–F over a wavelength region of 350–800 nm.

anomalously large intensity when compared to the normal octahedral spectrum shown in Fig. 1.

The theory and data given in the literature (Table I) for the spectrum of Ni^{2+} in a cubic field support the fact that the band at 400 nm should be about twice as intense as the one at 660 nm. On first impression one might hypothesize that distortion of the octahedron causes this effect for these two bands. However, the wavelength value determined here is a good deal smaller in magnitude than that expected for the $^3A_{2g}(F) \rightarrow {}^3T_{2g}(P)$ transition for Ni^{2+} in a distorted sixfold coordination since, as mentioned previously, distortion causes shifts of the bands toward even higher wavelengths.

An alternate spectral interpretation can be found in the assumption that a fraction of Ni^{2+} is in tetrahedral symmetry. In this case, the band near 660 nm must represent overlapping bands assigned to $^3T_1(F) \rightarrow {}^3T_1(P)$ (for Ni^{2+} tetrahedral) and $^3A_{2g}(F) \rightarrow {}^3T_{1g}(P)$ (for Ni^{2+} octahedral) transitions.

Qualitatively, the position and shape of the 660-nm band can be explained in the following fashion: if we assume that absorption bands in uv and visible spectrum are Gaussian (*9*), and if one superimposes four Gaussian curves, two corresponding to the experimental value of the Ni^{2+} tetrahedral doublet bands having a center of gravity near 625 nm, and two corresponding to those of the Ni^{2+} octahedral doublet having a center of gravity around 714 nm, a reconstructed band of intermediate value would be obtained. Thus, the observed band at 658 nm could actually arise as a combination of these four single transitions. The anomalously large intensity of this band, compared with the band in the region of 400 nm, can be attributed to the fact that band intensities in tetrahedral are larger than those in octahedral ones. Therefore, any Ni^{2+} which occurs in tetrahedral symmetry would greatly increase band intensity. It should be further added that optical spectrum profile for these Ni-phyllosilicates agrees well with results obtained with spinels, in which Ni^{2+} occupies both octahedral and tetrahedral sites (*11*).

Quantitatively this hypothesis can be tested using nonlinear regression analysis. Each of the component bands can be described by Gaussian functions of the form

$$A = A_{max}\, e^{-k(\nu-\nu_{max})2}$$

where

A = percent absorbance at any ν
A_{max} = percent absorbance at ν_{max}
k = the coefficient related to bandwidth (cm^2)
ν = wave number (cm^{-1})
ν_{max} = wave number at maximum absorption (cm^{-1}).

A computer program ((BMDP 3R)–Health Science Computing Facility, University of California, Los Angeles) which utilizes a weighted least squares best fit and Gauss–Newton iteration then selects best values for A_{max}, k, ν_{max}, having had, as inputs, a set of A and ν data over the entire energy range of interest. It should be recalled that the composite curve is being reconstructed with four Gaussian wavefunctions (those corresponding to two tetrahedral and two octahedral bands expected in the wavelength region of 550 to 800 nm. Given that each wavefunction has its own associated A_{max}, ν_{max}, and k constants, the computer attempts to solve for 12 unknowns using a range of input A, ν data sets.

The results of this mathematical reconstruction are shown in Figs. 4A–F. In each figure, the composite curve, reconstructed from the "best fit" wavefunctions shown in the figures, is illustrated by a continuous line with associated real A and ν values taken from Fig. 3. As mentioned previously, resolved tetrahedral bands appear at lower wavelength than resolved octahedral bands in all cases. Associated A_{max}, ν_{max}, and k

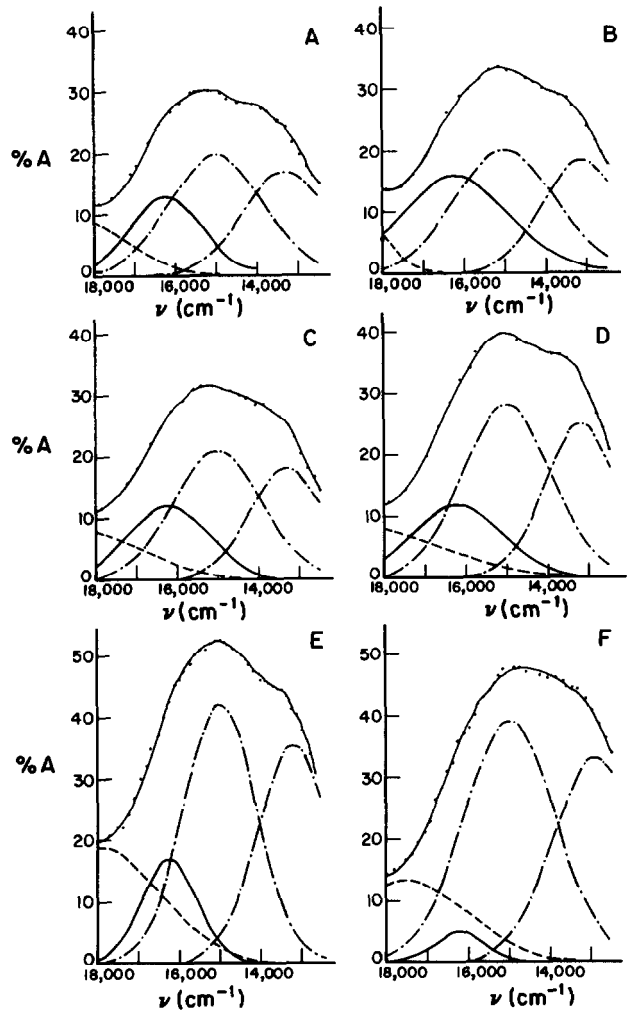

FIG. 4. Nonlinear regression analysis of uv reflectance spectra. Reflectance of composite spectra (over wavelengths from 500–800 nm) shown in Fig. 3 for mineral samples A–F corresponding to Figs. 3A–F, respectively. Composite theoretical curve ⟿ is fit by tetrahedral —, 2 octahedral - - - - -, and a low wavelength band --- due to tailing from very low wavelength octahedral peak shown in Fig. 3. Shown dots, superimposed upon the theoretical curve, are actual spectra data taken from Fig. 3.

constants for these functions are shown in Table IV. (ν values are from here on converted to λ for literature comparison). The resolved band, appearing at the lowest wavelength in all figures is not related physically to tetrahedral Ni^{2+} as it appears at too high an energy level. This band is predicated by the need to "fit" tailing produced by the even lower wavelength octahedral band at 390 nm. Indeed, there is always some tailing produced by this octahedral band which must be included in any curve fitting analysis.

Relative position and intensity of resolved octahedral bands at 667 and 758 nm closely compare to literature values for Ni^{2+} in MgO of 676 ± 7 and 746 ± 7 nm reported by Low (*10*). Although Ni^{2+} is

TABLE IV

RESULTS OF THE REGRESSION ANALYSIS AND RATIOS OF TETRAHEDRAL TO OCTAHEDRAL Ni^{2+}

Sample Fig. 4	A_{max}	k	ν_{max} (cm^{-1})	RMS[a]	n[b]	$\frac{S_{Ni^{2+}\,T}}{S_{Ni^{2+}\,Oc}}$
	19.5	38.6	15,000			
A	17.6	45.8	13,306	0.4	32	0.29
Fig. 4A	12.8	62.9	16,200			
	10.2	25.9	18,760			
	20.0	34.9	15,000			
B	18.2	54.9	13,126	0.3	27	0.49
Fig. 4B	15.6	28.3	16,200			
	10.5	92.0	18,760			
	21.0	42,3	15,000			
C	18.0	58.0	13,296	0.3	30	0.30
Fig. 4C	12.0	50.0	16,200			
	8.8	15.2	18,760			
	28.0	43.1	15,000			
D	25.0	63.6	13,176	0.3	30	0.24
Fig. 4D	11.6	40.2	16,200			
	8.5	11.3	18,760			
	42.0	62.4	15,000			
E	35.3	63.0	13,199	0.4	46	0.16
Fig. 4E	16.8	107.9	16,250			
	18.8	24.3	17,905			
	39.0	39.9	15,000			
F	33.0	46.7	12,914	0.4	37	0.04
Fig. 4F	5.0	135.1	16,250			
	13.3	21.9	17,555			

[a] RMS = Residual mean square.
[b] n = Number of cases.

bound not only by oxygen in nickel phyllosilicates, but also by OH, it is not surprising to find close agreement with the oxide spectrum due to the fact that O and OH ligands are not significantly different with respect to field strength. In addition, the intensity ratio $I_{667\,nm}/I_{758\,nm}$ of 1.3 agrees favorably with the 1.5 value obtained by Low (*10*).

Most importantly, however, it should be noted that all samples, (with the possible exception of sample F), show a band at 617 nm. The position of this band corresponds closely to that reported in the literature (Table I) for tetrahedrally coordinated nickel.

Even more information about the nature of these minerals can be gained by examining the ratio of peak areas of the resolved uv reflectance spectrum. By comparing the area underneath the peaks attributed to the Ni^{2+} tetrahedral with the total area of octahedral peaks some semiquantitative information about the Ni^{2+} tetrahedral versus octahedral character can be obtained (absolute quantitation is impossible due to uncertainty in extinction coefficients). From results shown in Table IV, it is obvious that a trend can be seen, the highest portion of tetrahedral Ni^{2+} being found in sample B which is the sample having the highest interlayer charge density as well. The peak area ratio decreases for samples A and C which correspond to 2 : 1 phyllosilicates but with negligible exchange capacity. This is followed by samples D and E, both 1 : 1 type phyllosilicates. The peak area ratio therefore closely matches the probability of finding Ni^{2+} tetrahedrally coordinated "sites." That is, one would expect a 2 : 1 phyllosilicate to have more tetrahedral substitutions than a 1 : 1. One also would expect that Ni^{2+} substitution in these samples to be a function of the exchangeable capacity and this can be seen by comparing the 2 : 1 samples A and C with B. Differences in peak area ratio can also be found between the amorphous coprecipitate sample and that same sample crystallized by hydrothermal reaction (sample E). Notice that crystallization increases the peak area ratio suggesting that this process increases the probability of finding Ni^{2+} tetrahedrally coordinated in the silica layer.

Further evidence for the presence of tetrahedral nickel in phyllosilicates can be found by comparing the Ni/Si atomic ratio for extremely well-crystallized willemsite (sample C) with respect to its theoretical stoichiometry (see Table II). In earlier studies involving nickeloan kerolite–pimelite minerals, deviations showing a higher content in tetrahedral and lower content in octahedral cations than that predicted by structural formulae have been interpreted with respect to $Ni(OH)_2$ and/or serpentine minerals being present as impurities (*2*). This possibility has been checked with analytical electron microscopy (thin film X-ray microanalysis). For all particles examined

with the microprobe, the nickel/silica ratio was constant with the exception of a few cases (very small particles) which only contained silica. This indicates that no $Ni(OH)_2$ impurities were present in spite of the fact that some amorphous silica was being observed. This evidence lends additional support to results from above, showing that, for sample C, a small amount of Ni^{2+} must be in the tetrahedral position.

Conclusion

This paper has presented both qualitative and semiquantitative data to indicate that Ni^{2+} can exist in tetrahedral coordination in phyllosilicates. By using uv reflectance spectroscopy and nonlinear regression analysis of spectral data, it has been possible to show that some Ni^{2+} is tetrahedrally coordinated in all phyllosilicates examined. Further support for this argument has been presented in the case of highly crystalline willemseite. Here, nickel would only be expected to exist in octahedral sheets and the atomic ratio of Ni/Si should be 0.75. Chemical analysis of this sample, on the other hand, gave a ratio of 0.82 supporting spectral evidence that some Ni^{2+}, even in this highly crystallized synthetic sample, is tetrahedrally coordinated. Although exchange capacity for Ni^{2+} substituted phyllosilicates can be expected to be small compared to exchange capacities in Al^{3+} and Fe^{3+} substituted phyllosilicates due to ion size constraints, we simply point out here that *some* Ni^{2+} substitution can occur. The fact that some tetrahedrally coordinated Ni^{2+} has been found in all phyllosilicates examined may help to explain the anomalous swelling capacity in some of these minerals. As is the case here, the one demonstrating the most clear swelling character, namely sample B, is also the sample having largest exchange capacity and the sample having the highest peak area ratio ($Ni^{2+}_{tetrahedral}/N^{2+}_{octahedral}$). In spite of the fact that similar charge related swelling phenomena could be alternatively attributed to vacancies in crystal structure, evidence presented here warrants a closer examination of tetrahedral nickel's role in the structure of phyllosilicates.

Acknowledgments

This work was performed at the Groupe de Physico-Chimie Minérale et de Catalyse, Place Croix du Sud 1, B1348 Louvain-la-Neuve, Belgium, under a research grant from Belgian Secretary of State for Scientific Policy (Services de la Programmation de la Politique Scientifique).

References

1. G. W. Brindley, D. L. Bish, and H. Wan, *Amer. Mineral.* **64,** 615 (1979).
2. G. W. Brindley, Bull. *Bur. Rech. Geol. Min. Fr. Ser. 2 Sect. 2* **3,** 233 (1978).
3. G. W. Brindley, and H. Wan, *Amer. Mineral.* **60,** 863 (1975).
4. G. W. Brindley and Pham Thi Hang, *Clay Clay Miner.* **21,** 27 (1973).
5. B. P. Strangham and S. Walkes, "Spectroscopy," Science Paperbooks, New York (1976).
6. F. S. Stone, *Bull. Soc. Chim. Fr. Ser. 5,* 820 (1966).
7. G. H. Faye, *Canad. Mineral.* **12,** 389 (1974).
8. Z. Maksimovic and D. L. Bish, *Amer. Mineral.* **63,** 484 (1978).
9. B. N. Figgis, "Introduction to Ligand Fields." Interscience, New York (1966).
10. W. Low, *Phys. Rev.* **109,** (2), 241 (1958).
11. V. D. Schmitz-Du Mont, H. Gossling, and H. Brokoff, *Z. Anorg. Allg. Chem.* **300,** 159 (1959).
12. B. J. Wood, *Amer. Mineral.* **59,** 244 (1974).
13. G. R. Rossman, R. D. Shannon, and K. Waring, *J. Solid State Chem.* **39,** 277–287 (1981).
14. G. A. Martin, A. Renouprez, G. Dalmai-Imelik, and B. Imelik, *Bull. Soc. Fr. Mineral. Cristallogr.* **94,** 1142 (1971).
15. F. Albert Cotton and Geoffrey Wilkinson, "Advanced Inorganic Chemistry." Wiley-Interscience, New York (1980).